Analysis of primary synchronous breast invasive ductal carcinoma and lung adenocarcinoma with next-generation sequencing: A case report

DI WU[1], JINYU YU[2], LIANG GUO[1], XIAOFEI WEI[1], ZHUANG TIAN[1] and XIUMEI DUAN[1]

Departments of [1]Pathology and [2]Urology, The First Hospital of Jilin University, Changchun, Jilin 130021, P.R. China

Received May 18, 2022; Accepted October 10, 2022

DOI: 10.3892/ol.2022.13604

Abstract. Multiple primary cancers (MPCs) have an increasing incidence rate due to the detection of early stages of cancer and the development of effective therapeutic strategies. MPCs are less common compared with metachronous cancers. Therefore, distinguishing synchronous primary tumors from metastasis and developing an individualized treatment strategy can be challenging. In the present study, the case of a 70-year-old female who was referred to The First Hospital of Jilin University (Changchun, China) with an enlarged left cervical lymph node and no other clinical manifestations is reported. Radiography revealed distinct lesions in the left breast, left cervical lymph node and bilateral lungs. Subsequently, a biopsy was performed in all three lesions and then each specimen was subjected to immunohistochemistry, fluorescence *in situ* hybridization, amplification refractory mutation system-PCR and next-generation sequencing (NGS). Disease-related enrichment of lymph node mutant genes and Gene Ontology Biological Process enrichment of breast, as well as lung, mutant genes were performed using the Database for Annotation, Visualization and Integrated Discovery. Based on the molecular assessment, the patient was finally diagnosed with breast invasive ductal carcinoma, primary lung adenocarcinoma and cervical lymph node metastatic lung adenocarcinoma. Since primary synchronous breast and lung cancer (SBLC) is rare, a molecular assessment, particularly using NGS, could provide important information for both the diagnosis and treatment of SBLC.

Correspondence to: Professor Xiumei Duan, Department of Pathology, The First Hospital of Jilin University, 1 Xinmin Street, Changchun, Jilin 130021, P.R. China
E-mail: xmduan@jlu.edu.cn

Key words: breast invasive ductal carcinoma, lung adenocarcinoma, next-generation sequencing, primary synchronous tumors, case report

Introduction

Multiple primary cancers (MPCs) refer to two or more primary malignancies occurring simultaneously or successively in the same patient. The frequency of MPCs varies between 2 and 17%, depending on different criteria (1). The International Association of Cancer Registries and International Agency for Research on Cancer recommend a time-lapse of 6 months to distinguish between synchronous and metachronous MPCs (2). Synchronous MPCs are less common compared with metachronous MPCs. In a retrospective study that included 8,204 patients with breast cancer with MPCs, 4 patients suffered from synchronous cancer in the lungs or thorax, thus suggesting that the morbidity of synchronous breast and lung cancer (SBLC) was <0.05% in patients with breast cancer and MPCs (3). Another study reported a slightly higher percentage (0.56%), since among 1,066 patients with breast cancer, 6 were diagnosed with SBLC (4). Besides, SBLC cases are commonly reported as case reports lacking systemic analysis. The clinical symptoms of synchronous MPCs may overlap with each other, thus resulting in the masking of the clinical manifestations of the second primary cancer. Therefore, improving the understanding of synchronous MPCs is of great importance for avoiding misdiagnosis or missed diagnosis. Next-generation sequencing (NGS) provides significant information in terms of the diagnosis, treatment and potential etiological clues of the disease. In the present study, the case of a patient who initially presented with breast cancer and metastatic lesions in the cervical lymph nodes is reported. Further evaluation revealed the presence of synchronous primary lung adenocarcinoma. Therefore, NGS across 689 genes associated with the development, treatment and prognosis of solid tumors for the breast, lung and lymph node lesions was performed aiming to raise awareness of SBLC in genetics. To the best of our knowledge, there is no similar case previously reported in the literature.

Case report

General clinical conditions. A 70-year-old female was first referred to The First Hospital of Jilin University (Changchun, China) due to enlarged lymph nodes in the left side of the neck in January 2017. The patient was healthy prior to the onset of the this symptom. The patient's living and working conditions were of good quality, and there was no tobacco, alcohol

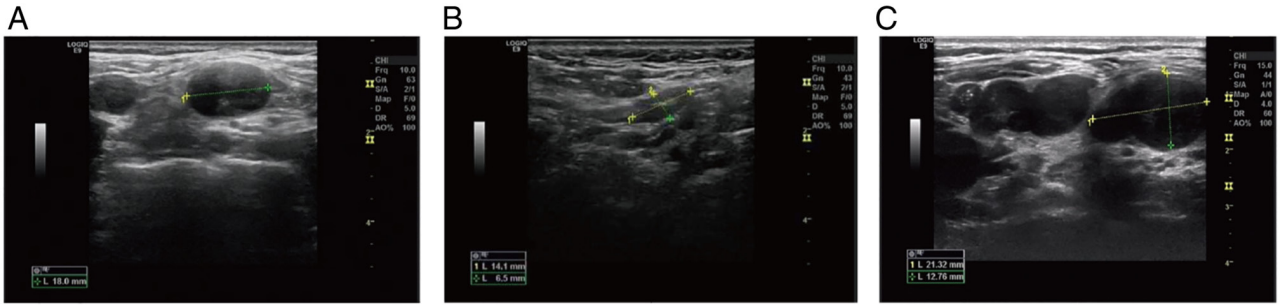

Figure 1. Ultrasound images of the patient. (A) Enlarged lymph nodes in the left neck in January 2017. (B) The cervical lymph nodes were reduced during therapy in January 2019. (C) The cervical lymph nodes were enlarged for the second time in March 2020.

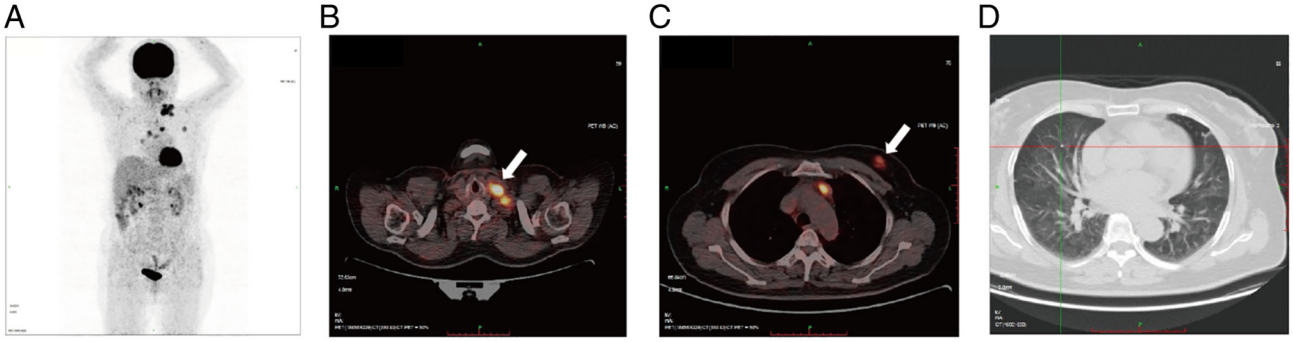

Figure 2. PET-CT images of the patient. (A) Whole-body coronal PET-CT image. (B) FDG uptake (arrow) in the left breast lesion. (C) FDG uptake (arrow) in the left cervical lymph nodes. (D) Small nodule in the right lung without metabolic activity. PET-CT, positron emission tomography-computed tomography; FDG, fluorodeoxyglucose.

or drug addiction. The patient had no anemia, inflammatory syndrome or other clinical manifestations. Tumor marker detection showed no abnormalities.

Methods. Ultrasound of the neck and mammary gland, as well as positron emission tomography-computed tomography (PET-CT), was performed when the patient was first admitted to the hospital. A left breast and left cervical lymph node biopsy were then performed for diagnostic purposes. When the disease progressed 62 months after her first visit, the patient underwent a CT scan of the lungs and a biopsy of the right lung nodule. The breast, lymph node and lung specimens were fixed with 10% formalin at room temperature for 24 h, then embedded with paraffin and assessed for immunohistochemical examination, gene variations and fluorescence *in situ* hybridization (FISH) for further diagnosis and treatment.

The sections (5 μm) for immunohistochemical examination were heated at 70˚C for 30 min in an electric thermostatic drying oven (Shanghai Yiheng Scientific Instrument Co., Ltd.), dewaxed with xylene at room temperature, rehydrated in a descending alcohol series at room temperature, and endogenous peroxidase activity was blocked using 3% H_2O_2 at room temperature for 10 min, followed by blocking with 10% normal goat serum (ab7481; Abcam) at 37˚C for 30 min. Subsequently, the sections were incubated with primary antibodies stock solution (undiluted), including CK7 (MAB-0828; Fuzhou Maixin Biotech Co., Ltd.), Napsin A (MAB-0704; Fuzhou Maixin Biotech Co., Ltd.), TTF-1 (MAB-0677; Fuzhou Maixin Biotech Co., Ltd.), ER (Kit-0012; Fuzhou Maixin Biotech Co., Ltd.), PR (Kit-0013; Fuzhou Maixin Biotech Co., Ltd.), HER2 (Kit-0043; Fuzhou Maixin Biotech Co., Ltd.), CA15-3 (MAB-0241; Fuzhou Maixin Biotech Co., Ltd.) and GCDFP15 (MAB-0230; Fuzhou Maixin Biotech Co., Ltd.) antibodies at 37˚C for 2 h. Finally, the sections were incubated with secondary antibody stock solution (undiluted) at 37˚C for 30 min and dyed with DAB for 5 min using MaxVision III ultra DAB (Kit-0038; Fuzhou Maixin Biotech Co., Ltd.). The sections were then observed under a light microscope (Olympus Corporation).

Amplification refractory mutation system-PCR (ARMS-PCR) was performed in nine genes. DNA and RNA were extracted from tissues using a formalin-fixed paraffin-embedded (FFPE) DNA/RNA Kit (cat. no. 20150082; Amoy Diagnostics Co., Ltd.). ARMS-PCR was performed using a Multi-Gene Mutations Detection Kit (cat. no. 20183401043; Amoy Diagnostics Co., Ltd.) and detected using Mx3000P Real-Time QPCR System (Agilent Technologies, Inc.), using the negative and positive controls from the kit as the quality control. The thermocycling conditions were set up according to the manufacturer's instructions (stage 1, 42˚C for 5 min, 95˚C for 5 min for 1 cycle; stage 2, 95˚C for 25 sec, 64˚C for 20 sec, 72˚C for 20 sec for 10 cycles; stage 3, 93˚C for 25 sec, 60˚C for 35 sec, 72˚C for 20 sec for 36 cycles). The cycle threshold of each reaction was read directly on the Mx3000P Real-Time QPCR System and interpreted according to the positive threshold defined in the manual.

NGS was performed in 689 genes. The sequencing was performed by BGI Genomics using a QIAamp DNA FFPE

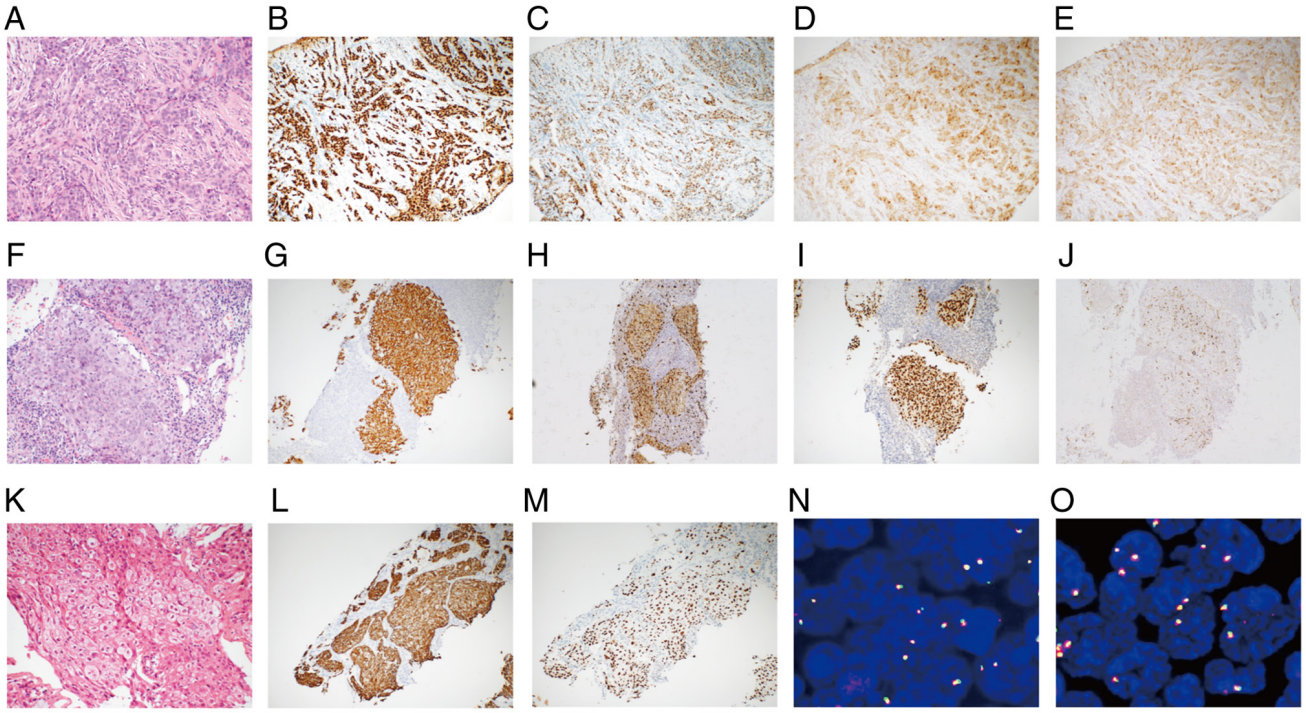

Figure 3. Histopathological, immunohistochemical and fluorescence *in situ* hybridization characterization of the breast, lymph node and lung lesions. (A) H&E staining of the breast lesion (magnification, x200). (B-E) Immunohistochemical expression of (B) estrogen receptor, (C) progesterone receptor, (D) gross cystic disease fluid protein 15 and (E) CA15-3 in the breast lesion (magnification, x100). (F) H&E staining of the lymph node lesion (magnification, x200). (G-J) Immunohistochemical expression of (G) CK7, (H) Napsin A, (I) TTF1 and (J) CA15-3 in the lymph node lesion (magnification, x100). (K) H&E staining of the lung lesion (magnification, x200). (L and M) Immunohistochemical expression of (L) CK7 and (M) TTF1 in the lung lesion (magnification, x100). (N) *KIF5B-RET* fusions in the lymph node lesion (magnification, x1,000). (O) *KIF5B-RET* fusions in the lung lesion (magnification, x1,000). (A-J) July 2017. (K-M) November 2021. (N and O) August 2022. H&E, hematoxylin and eosin; CK, cytokeratin; TTF1, thyroid transcription factor 1; CA15-3, cancer antigen 15-3; KIF5B, kinesin family member 5B; RET, ret proto-oncogene.

Table I. Immunohistochemistry results in the breast, lymph node and lung.

Immunohistochemistry marker	Breast	Lymph node	Lung
CK7	NA	+	+
Napsin A	NA	+	-
TTF1	-	+	+
ER	+ (90%)	-	-
PR	+ (70%)	-	-
HER2[a]	2+	0	0
CA15-3	+	+	NA
GCDFP15	+	-	NA

[a]Immunohistochemistry grade according to the American Society of Clinical Oncology/College of American Pathologists Clinical Practice Guideline (12). CK7, cytokeratin 7; TTF1, thyroid transcription factor-1; ER, estrogen receptor; PR, progesterone receptor; HER-2, human epidermal growth factor receptor 2; CA15-3, cancer antigen 15-3; GCDFP15, gross cystic disease fluid protein 15; NA, not available.

Tissue Kit (cat. no. 56404; Qiagen Inc.) and a MagPure Buffy Coat DNA Midi KF Kit (cat. no. D3537-02; Magen Biotechnology Co., Ltd.) for preparing the DNA sample. Agarose gel electrophoresis was used to verify the quality of the processed samples. The type of sequencing was 100 bp paired end and was performed using an MGISEQ-2000RS NGS Kit (cat. no. 1000012554; BGI Genomics). The loading concentrations of the final library were 81.2, 33.8 and 85.4 ng/μl for the breast, lymph node and lung specimens, respectively, as measured by a Qubit fluorometer (Thermo Fisher Scientific, Inc.).

FISH was performed in the lung and lymph node tissue specimens to detect ret proto-oncogene (*RET*) fusions as a gold standard. After dewaxing with xylene, FFPE lung and lymph node tissue sections (3 μm) were pretreated through proteolytic digestion using FFPE FISH PreTreatment Kit 1 (cat. no. KA2691; Abnova). Denaturation (75˚C for 5 min), hybridization (37˚C for 16 h), washes and counterstaining were performed using a kinesin family member 5B (KIF5B)/RET SY Translocation FISH Probe Kit (cat. no. FT0006; Abnova) according to the manufacturer's instructions. The sections were then detected under a fluorescence microscope at x1,000 magnification (Olympus Corporation).

Results. The ultrasound of the left side of the neck revealed numerous hypoechoic areas, several of which were fused with each other, without a normal cortex and medulla structure. The border was clear and the internal echo was uneven. Some of these areas exhibited a strong mottling echo (Fig. 1). The ultrasound of the mammary gland revealed an 11.0x6.6-mm anechoic mass on the lateral side of the left mammillary papilla. The boundary was clear and the shape was regular.

Table II. Gene variations in the breast, lung and lymph node.

A, Breast

Gene	Variation	Transcript	Mutation abundance or copy number
MTOR	p.E1799K(c.5395G>A)	NM_004958.3	0.43%
EGFR	p.T790M(c.2369C>T)	NM_005228.3	0.42%
IDH2	p.R140W(c.418C>T)	NM_002168.2	0.40%
MCL1	copy number amplification	NM_021960.4	4.82
HLA-A	p.Q250Hfs*47(c.750_751delGGinsC)	NM_002116.7	23.84%
RBM10	p.S288*(c.863C>G)	NM_005676.4	1.24%
PMS1	p.E543*(c.1627G>T)	NM_000534.4	0.93%
MAP2K1	p.D67N(c.199G>A)	NM_002755.3	0.55%
SMARCA4	p.T910M(c.2729C>T)	NM_001128849.1	0.49%
ERBB2	p.R896C(c.2686C>T)	NM_004448.2	0.42%
STK11	p.D194N(c.580G>A)	NM_000455.4	0.40%
TRRAP	p.H913Q(c.2739C>G)	NM_003496.3	23.37%
CDC27	p.H615N(c.1843C>A)	NM_001114091.1	14.87%
CTNND2	p.V428I(c.1282G>A)	NM_001332.2	10.37%
ELF3	p.S266N(c.797G>A)	NM_001114309.1	10.28%
MUC6	p.T1411K(c.4232C>A)	NM_005961.2	3.78%
AMER1	p.V663L(c.1987G>C)	NM_152424.3	3.12%
MUC16	p.T11030A(c.33088A>G)	NM_024690.2	2.30%
PRKD1	p.P35_A36insGP(c.101_106dupGGCCCG)	NM_002742.2	1.79%
EP300	p.Q2108L(c.6323A>T)	NM_001429.3	1.40%
CIC	p.G525A(c.1574G>C)	NM_015125.3	1.33%
MUC16	p.L11003I(c.33007C>A)	NM_024690.2	1.24%
MDC1	p.C1599G(c.4795T>G)	NM_014641.2	1.15%
MDC1	p.E1380D(c.4140G>C)	NM_014641.2	1.09%
RAD50	p.Y569K(c.1705_1707delTATinsAAA)	NM_005732.3	0.97%
RAD50	p.F570Y(c.1709T>A)	NM_005732.3	0.95%
PMS1	p.N542H(c.1624A>C)	NM_000534.4	0.94%
TFE3	p.R196L(c.587G>T)	NM_006521.4	0.90%
MDC1	p.S1508P(c.4522T>C)	NM_014641.2	0.86%
ADGRA2	p.P395R(c.1184C>G)	NM_032777.9	0.86%
SPRED1	p.E373Q(c.1117G>C)	NM_152594.2	0.73%
EPHA2	p.N831I(c.2492A>T)	NM_004431.3	0.68%

B, Lung

KIF5B-RET	Fusion	NM_004521.2-NM_020975.4	27.41%
MYC	Copy number amplification	NM_002467.4	4.95
NSD1	Copy number amplification	NM_022455.4	4.82
ATAD2	Copy number amplification	NM_014109.3	4.68
CCNE1	Copy number amplification	NM_001238.2	4.29
PTCH1	p.P24L(c.71C>T)	NM_000264.3	17.36%
MSH4	p.L399V(c.1195C>G)	NM_002440.3	13.32%
KMT2C	p.R973G(c.2917A>G)	NM_170606.2	12.26%
KMT2C	p.R886C(c.2656C>T)	NM_170606.2	10.24%

C, Lymph node

KIF5B-RET	Fusion	NM_004521.2-NM_020975.4	5.46%

Table II. Continued.

C, Lymph node			
TP53	p.P301Qfs*44(c.902delC)	NM_000546.5	0.31%
MCL1	Copy number amplification	NM_021960.4	5.71
HLA-A	p.Q250Hfs*47(c.750_751delGGinsC)	NM_002116.7	19.18%
PTPRS	p.R979*(c.2935C>T)	NM_002850.3	0.73%
STAT5A	c.1169+1G>A	NM_003152.3	0.65%
MYC	Copy number amplification	NM_002467.4	5.64
ZNF217	Copy number amplification	NM_006526.2	5.19
CDKN1B	Copy number amplification	NM_004064.3	5.11
SRSF2	Copy number amplification	NM_003016.4	4.83
DAXX	Copy number amplification	NM_001141970.1	4.81
KLF6	Copy number amplification	NM_001300.5	4.57
CDC27	p.H615N(c.1843C>A)	NM_001114091.1	17.01%
MSH4	p.L399V(c.1195C>G)	NM_002440.3	12.24%
PTCH1	p.P24L(c.71C>T)	NM_000264.3	8.90%
KMT2A	p.R2707W(c.8119C>T)	NM_001197104.1	1.01%
NUDT18	p.P153L(c.458C>T)	NM_024815.3	0.78%
DOCK2	p.S1170L(c.3509C>T)	NM_004946.2	0.77%
BCL6	p.R40C(c.118C>T)	NM_001706.4	0.76%
POLG	p.R869Q(c.2606G>A)	NM_002693.2	0.75%
ZNRF3	p.E775K(c.2323G>A)	NM_001206998.1	0.74%
PRDM1	p.P467L(c.1400C>T)	NM_001198.3	0.72%
TRRAP	p.V3197M(c.9589G>A)	NM_003496.3	0.71%
SLX4	p.R1062H(c.3185G>A)	NM_032444.2	0.70%
KLHL6	p.E568K(c.1702G>A)	NM_130446.2	0.61%
RECQL4	p.R780W(c.2338C>T)	NM_004260.3	0.61%

The asterisk indicates that the mutational site is in the non-coding region.

PET-CT showed that the aforementioned lesions in the breast and neck were metabolically active (Fig. 2). The right lung and upper lobe of the left lung presented with several small nodules without metabolic activity, thus indicating inflammation (Fig. 2). Pathological morphology and immunohistochemical examination of the left breast suggested breast invasive ductal carcinoma (Table I; Fig. 3). In addition, morphology in the left cervical lymph node revealed a poorly differentiated tumor in the lymphoid tissue and immunohistochemical results were of little help in identifying the source of the tumor (Table I; Fig. 3). Therefore, the left cervical lymph node tissue specimens and peripheral blood were sent for mutational analysis. The analysis showed that the cells expressed wild-type *EGFR*, with no *ALK* or *ROS1* gene rearrangements. Based on the aforementioned results, the cervical lymph node lesions were considered as metastases arising from breast cancer. The patient was treated with letrozole (2.5 mg once a day; endocrine therapy) from February 2017 for breast cancer until March 2020. During therapy, the neck mass was significantly reduced in size (Fig. 1). In March 2020, the cervical lymph nodes were enlarged for the second time, thus indicating disease progression (Fig. 1). Therefore, the patient was treated with an adjusted treatment strategy with a combination of palbonix (125 mg once a day) and fulvestrant (250 mg once a month) until November 2021, when they were diagnosed with enlarged bilateral pulmonary nodules. The patient was then treated with chidamide (30 mg twice a week) plus exemestane (25 mg once a day) for the next month, until a CT scan showed that the bilateral pulmonary nodules were further enlarged. This finding indicated disease progression for the third time. A right lung biopsy revealed a poorly differentiated carcinoma and the immunohistochemistry results supported the diagnosis of primary lung adenocarcinoma (Table I; Fig. 3). Next, the patient was treated with albumin-bound paclitaxel (400 mg was administered twice 3 weeks apart) from January 2022 for both breast and lung cancer, and has survived with tumors for 8 months up to the time of writing the study.

Gene detection and analysis. The breast, lymph node and lung tissue specimens were evaluated for gene mutations and fusions in nine genes using ARMS-PCR. The analysis revealed *RET* gene fusions, without *EGFR*, *HER2*, *KRAS*, *NRAS*, *BRAF* and *PIK3CA* gene mutations, or *ALK* and *ROS1* gene fusions, in both the lung and lymph node specimens. Neither gene mutations nor fusions were detected in the breast specimen. Subsequently, NGS across 689 genes in each specimen was performed. The Database for Annotation, Visualization and Integrated Discovery Bioinformatics

Table III. Disease enrichment terms of varied genes from the lymph node specimen.

Term	P-value	Genes	FDR
Lymphoma	$5.36x10^{-6}$	*CDKN1B, BCL6, MYC, HLA-A, TP53*	0.004937
Bladder cancer	$1.95x10^{-4}$	*RECQL4, RET, CDKN1B, BCL6, MYC, TP53, POLG*	0.087424
Lung cancer	$3.61x10^{-4}$	*RET, KLF6, CDKN1B, BCL6, MYC, HLA-A, TP53*	0.087424
Head and neck cancer	$4.72x10^{-4}$	*RECQL4, CDKN1B, HLA-A, TP53*	0.087424
Chronic renal failure|Kidney Failure, Chronic	$5.34x10^{-4}$	*CDKN1B, BCL6, MYC, MSH4, HLA-A, PRDM1, TP53, POLG*	0.087424
Lymphoma, B-Cell|Lymphoma, Follicular|Lymphoma, Large B-Cell, Diffuse	$5.70x10^{-4}$	*BCL6, MYC, TP53*	0.087424
Pharmacogenetic studies	$7.58x10^{-4}$	*KMT2A, MYC, HLA-A, TP53*	0.090843
Leukemia	$8.21x10^{-4}$	*CDKN1B, KMT2A, HLA-A, TP53*	0.090843
Precursor Cell Lymphoblastic Leukemia-Lymphoma	$8.88x10^{-4}$	*STAT5A, DAXX, HLA-A, TP53*	0.090843

FDR, false discovery rate.

Table IV. GO-biological process enrichment terms of varied genes from the breast and lung specimens.

A, Breast

Term	P-value	Genes	FDR
GO:0046777~protein autophosphorylation	$9.03x10^{-5}$	*STK11, ERBB2, PRKD1, EGFR, MTOR*	$2.33x10^{-2}$
GO:0018107~peptidyl-threonine phosphorylation	$1.16x10^{-4}$	*MAP2K1, STK11, PRKD1, MTOR*	$2.33x10^{-2}$
GO:0033674~positive regulation of kinase activity	$1.26x10^{-4}$	*RAD50, ERBB2, EGFR, EPHA2*	$2.33x10^{-2}$
GO:1904837~beta-catenin-TCF complex assembly	$6.89x10^{-4}$	*TRRAP, EP300, SMARCA4*	$6.65x10^{-2}$
GO:0070372~regulation of ERK1 and ERK2 cascade	$6.89x10^{-4}$	*ERBB2, EGFR, EPHA2*	$6.65x10^{-2}$
GO:0018108~peptidyl-tyrosine phosphorylation	$7.19x10^{-4}$	*MAP2K1, ERBB2, EGFR, EPHA2*	$6.65x10^{-2}$
GO:0045765~regulation of angiogenesis	$8.94x10^{-4}$	*ADGRA2, ERBB2, EPHA2*	$7.08x10^{-2}$
GO:1901796~regulation of signal transduction by p53 class mediator	$11.45x10^{-4}$	*STK11, RAD50, EP300, MTOR*	$7.94x10^{-2}$

B, Lung

Term	P-value	Genes	FDR
GO:0045893~positive regulation of transcription, DNA-templated	$1.38x10^{-6}$	*RET, CCNE1, MYC, NSD1, PTCH1, ATAD2*	$2.86x10^{-4}$

GO, Gene Ontology.

Resource (v2022q3; https://david.ncifcrf.gov/) was utilized to assess disease-related enrichment (P<0.05; FDR<0.1) of lymph node mutant genes and Gene Ontology Biological Process (GO BP) enrichment (P<0.05; FDR<0.1) of the

breast mutant genes, as well as lung mutant genes, which were identified based on NGS results. The analysis identified 26 somatic alterations in 27 genes in the lymph node specimen, 32 in 27 genes in the breast specimen and nine somatic mutations in nine genes in the lung specimen (Table II). No germline mutations were detected in any specimen. *RET* gene fusions were identified in both the lung and lymph node specimens. Lymph node mutated genes were enriched in nine terms and the top three were 'lung cancer', 'lymphoma' and 'bladder cancer' [Table III; P<0.05; false discovery rate (FDR)<0.1]. In addition, the mutated genes in the lung specimen, including *RET*, *CCNE1*, *MYC*, *NSD1*, *PTCH1* and *ATAD2*, were enriched in the 'positive regulation of transcription, DNA-templated' (Table IV; P<0.05; FDR<0.1). Finally, breast mutated genes, including *EGFR*, *STK11*, *ERBB2*, *PRKD1*, *MTOR*, *MAP2K1*, *RAD50* and *EPHA2*, were enriched in eight significant terms. The top three were 'protein autophosphorylation', 'peptidyl-threonine phosphorylation' and 'positive regulation of kinase activity' (Table IV; P<0.05; FDR<0.1).

Discussion

When dealing with MPCs, distinguishing synchronous primary tumors from metastatic ones can be challenging but significant, since there are different treatment strategies for each type of cancer. Although no metastatic lung tumor from breast cancer has been identified as pure ground glass opacity (5), more than one-half of primary lung cancer cases are classified as partly or purely solid tumors based on pulmonary CT scan (4). Therefore, it is difficult to distinguish a primary lung cancer from a metastatic tumor based on CT imaging features alone. Therefore, pathological analysis is considered the gold standard for the diagnosis. The majority of SBLC cases are breast invasive ductal carcinoma with lung adenocarcinoma (4). However, when both tumors show a poorly differentiated morphology, it is difficult to identify their origin. Although immunohistochemistry can offer some useful clues, due to the existence of triple-negative breast cancer, estrogen receptor-, progesterone receptor- and human epidermal growth factor receptor 2-negative results in lung lesions cannot completely exclude the possibility of breast cancer metastasis. Thyroid transcription factor-1 and Napsin A are two specific immunological markers for lung adenocarcinoma. However, their negative expression cannot completely exclude the possibility of primary lung adenocarcinoma. Therefore, the application of immunohistochemistry in the differential diagnosis is limited. NGS can reveal whether the lesions show the same clonality and therefore a primary tumor can be distinguished from metastases. In the present case, at the time of the initial visit, the lung nodules were small and showed low metabolism on the PET-CT scan. The mutational analysis of *EGFR*, *ALK* and *ROS1* in the lymph nodes revealed no common gene mutations or fusions associated with lung cancer. Therefore, the lymph node lesions were considered as metastases from breast cancer and the patient was treated with endocrine therapy. However, NGS was performed after disease progression and the mutated genes in the lymph node specimen were enriched in 'lung cancer', but not in breast cancer. Furthermore, although it has been reported that *RET* rearrangements are driver factors in several types of human cancer (6), in the present study, the *KIF5B-RET* fusion was only detected in the lung and lymph node specimens, but not in the breast specimens. Based on the aforementioned findings, it was hypothesized that the lymph node lesion was metastasis from the lung, thus indicating that the lung cancer was concomitant with the breast cancer. Although, it cannot be denied that histology, immunohistochemistry and radiological examination are useful in the differential diagnosis of SBLC, NGS displays a more significant value in determining the source of the tumor and in the early diagnosis of the second primary tumor.

The treatment of MPCs depends on the respective stage and aggressiveness of each primary cancer. The treatment of the more aggressive cancer precedes that of the other (7). Sometimes both types of cancer can be treated simultaneously, and therefore concomitant surgery for both breast and lung cancer is considered as a feasible and safe approach (8). Although the female patient in the present study suffered from synchronous MPC, lung cancer was diagnosed 3 years after the first visit and the lymph node lesion was reduced in size during endocrine therapy. The present study demonstrated that endocrine therapy for breast cancer was also effective for the metastatic cervical lymph nodes and could regulate the progression of lung cancer in the early stages of the disease. This finding was consistent with previous studies suggesting that the short-term use of hormone replacement therapy and oral contraceptives could significantly reduce the occurrence of lung cancer. However, long-term and continuous use could enhance the risk of lung cancer (9). The treatment strategy for SBLC should be individualized and based on multidisciplinary discussions.

Although several possible mechanisms for multiple primary breast and lung cancers have been suggested (1,2), some of the risk factors, such as radiotherapy and endocrine therapy, cannot explain the development of synchronous cancers. NGS provides significant information not only for the diagnosis and treatment, but also for the possible etiology of the disease. GO BP enrichment analysis of lung mutated genes revealed that the 'positive regulation of transcription, DNA-templated' was associated with lung cancer based on the NGS results. In addition, *KIF5B-RET* fusions were detected in both the lung and lymph node specimens. *KIF5B-RET* fusions are present in 1-2% of lung adenocarcinomas. It has been reported that the fusion transcripts of *KIF5B-RET* are likely to form a homodimer through the coiled coil domain of *KIF5B*, thus resulting in the aberrant phosphorylation of *RET* kinase (10). Similarly, the results also identified 'protein phosphorylation' as a significantly enriched term in the breast GO BP. The top three significantly enriched terms were 'protein autophosphorylation', 'peptidyl-threonine phosphorylation' and 'positive regulation of kinase activity'. *EGFR* T790M mutation was detected in the breast specimen by NGS, but not by ARMS-PCR. We hypothesize that this discrepancy may be due to the low mutation abundance (0.42% in NGS), which was below the lower limit of detection in ARMS-PCR. T790M is a common acquired mutation in patients with non-small cell lung cancer (NSCLC) initially treated with an *EGFR* tyrosine

kinase inhibitor (11). Although the primary T790M mutation is commonly identified in NSCLC, reports of this mutation in breast cancer are rare. In view of the fact that in the current case report breast cancer was accompanied by lung cancer, whether the occurrence of T790M was a random phenomenon or it was closely associated with the occurrence of SBLC should be further investigated in more cases.

In conclusion, the diagnosis and treatment of SBLC remains a challenge due to the lack of specific screening and well-established treatment guidelines. NGS could provide more detailed information for the diagnosis and treatment of SBLC. In addition, based on a large sample size, NGS could provide the possible underlying mechanisms of SBLC in the future. Nevertheless, further research is needed to increase our understanding in this area, while multidisciplinary discussion on individualized management is also required.

Acknowledgements

Not applicable.

Funding

This study was supported by the Norman Bethune Medical Engineering and Instrument Center Foundation (grant no. BQEGCZX2021020), the Department of Science and Technology of Jilin Province (grant no. 20200201434JC) and 12th Youth Development Foundation of the First Hospital of Jilin University (grant no. JDYY11202130).

Availability of data and materials

The dataset used and/or analyzed during the current study are available from the corresponding author on reasonable request.

Authors' contributions

XD designed and guided the paper. XD and DW confirm the authenticity of all the raw data. DW analyzed the data and wrote the manuscript. JY obtained PET-CT images. LG was responsible for pathological diagnosis and obtained pathological images. XW and ZT performed the experiments. All authors commented on the manuscript. All authors read and approved the final manuscript.

Ethics approval and consent to participate

This study was granted an exemption from requiring ethics approval from the Ethics Committee of Jilin University (Changchun, China).

Patient consent for publication

The patient provided written informed consent for the publication of any associated data and accompanying images.

Competing interests

The authors declare that they have no competing interests.

References

1. Vogt A, Schmid S, Heinimann K, Frick H, Herrmann C, Cerny T and Omlin A: Multiple primary tumours: Challenges and approaches, a review. ESMO Open 2: e000172, 2017.
2. Copur MS and Manapuram S: Multiple primary tumors over a lifetime. Oncology (Williston Park) 33: 629384, 2019.
3. Lee J, Park S, Kim S, Kim J, Ryu J, Park HS, Kim SI and Park BW: Characteristics and survival of breast cancer patients with multiple synchronous or metachronous primary cancers. Yonsei Med J 56: 1213-1220, 2015.
4. Shoji F, Yamashita N, Inoue Y, Kozuma Y, Toyokawa G, Hirai F, Ito K, Tagawa T, Okamoto T and Maehara Y: Surgical resection and outcome of synchronous and metachronous primary lung cancer in breast cancer patients. Anticancer Res 37: 5871-5876, 2017.
5. Tanaka K, Shimizu K, Ohtaki Y, Nakano T, Kamiyoshihara M, Kaira K, Rokutanda N, Horiguchi J, Oyama T and Takeyoshi I: Diagnosis and surgical resection of solitary pulmonary nodules in patients with breast cancer. Mol Clin Oncol 1: 117-123, 2013.
6. Takahashi M, Kawai K and Asai N: Roles of the RET Proto-oncogene in cancer and development. JMA J 3: 175-181, 2020.
7. Tanawade P, Misra S, Yathiraj P and Agarwal JP: A rare case of multicentric carcinoma left breast synchronous with carcinoma right lung: Therapeutic challenge in radiotherapy. J Cancer Res Ther 11: 665, 2015.
8. Mohamed S, Jawad F, Darr A, Christensen TD and Steyn R: Synchronous primary lung and breast carcinoma removed via a single incision. J Surg Case Rep 2020: rjz348, 2020.
9. Pesatori AC, Carugno M, Consonni D, Hung RJ, Papadoupolos A, Landi MT, Brenner H, Müller H, Harris CC, Duell EJ, *et al*: Hormone use and risk for lung cancer: A pooled analysis from the international lung cancer consortium (ILCCO). Br J Cancer 109: 1954-1964, 2013.
10. Kohno T, Ichikawa H, Totoki Y, Yasuda K, Hiramoto M, Nammo T, Sakamoto H, Tsuta K, Furuta K, Shimada Y, *et al*: KIF5B-RET fusions in lung adenocarcinoma. Nat Med 18: 375-377, 2012.
11. Li W, Qiu T, Guo L, Ling Y, Gao Y, Ying J and He J: Primary and acquired EGFR T790M-mutant NSCLC patients identified by routine mutation testing show different characteristics but may both respond to osimertinib treatment. Cancer Lett 423: 9-15, 2018.
12. Wolff AC, Hammond MEH, Allison KH, Harvey BE, Mangu PB, Bartlett JMS, Bilous M, Ellis IO, Fitzgibbons P, Hanna W, *et al*: Human epidermal growth factor receptor 2 testing in breast cancer: American society of clinical oncology/college of American pathologists clinical practice guideline focused update. Arch Pathol Lab Med 142: 1364-1382, 2018.